ISSN (Online) 2395-2717

International Journal of Engineering Research in Electrical and Electronic Engineering (IJEREEE)
Vol 4, Issue 3, March 2018

Stability Analysis of Indirect Vector Controlled Induction Motor Drive

[1] Santoshi R. Gawande, [2] Dr. Shubhangi.S.Ambekar, [3] Dr. Sudha Shrikant
Department of Electrical Engineering
K.D.K. College of Engineering Nagpur India.

***Abstract*: -- The effects of the induction motors parameters on the stability of driving systems operating at variable frequency are analyzed in this paper with the help of conventional method using computer simulation. In this paper, Nyquist stability criterion method is presented. The poles and zeros of the transfer functions for the rotor speed are calculated to investigate the influences of the controller parameters and motor parameters. The drive system shows the instability of lower values of frequency. Stability of induction motor in vector control depends on parameter variation. Changes in stator and rotor resistances have an effect on stability analysis of vector controlled induction motor. The indirect vector controlled induction motor is modeled and simulated using MATLAB and various results have observed to check the effect on the stability of the drive for changes in the parameters offering the regions of stability.**

Keywords: Induction motor control, Inverter, Indirect vector control, Parameter variation.

I. NOMENCLATURE

λ_r	Resultant rotor flux linkage
ω_{sl}	Slip speed
i^e_{ds}	Referred direct axis current
i^e_{qr}	Referred quadrature axis current
ω_s	Electrical stator frequency
ω_r	Electrical rotor speed
T_r	Rotor time constant
f_c	Switching frequency
p	Differential operator
P	Number of poles
$i^*_{as}, i^*_{bs}, i^*_{cs}$	Stator abc current commands

λ_r	Resultant rotor flux linkage
ω_{sl}	Slip speed
i^e_{ds}	Referred direct axis current
i^e_{qr}	Referred quadrature axis current
ω_s	Electrical stator frequency
ω_r	Electrical rotor speed
T_r	Rotor time constant
f_c	Switching frequency
p	Differential operator
P	Number of poles
$i^*_{as}, i^*_{bs}, i^*_{cs}$	Stator abc current commands

L_m	Mutual inductance per phase
L_r	Stator referred rotor self inductance per phase
R_r	Referred rotor resistance per phase
λ^e_{qr}	Quadrature axis flux linkages
λ^e_{dr}	Direct axis flux linkages

II. IMPLIMENTATION SETUP

Voltage controlled voltage source inverters are widely used in power supplies, power quality controllers, renewable energy, marine and military applications [1]. Three phase induction motors occupy an extremely high priority in the industrial applications world wide. Due to their ruggedness and less maintenance requiring capabilities, they are replacing the conventional dc motor from many areas viz cranes, locomotives etc. Adding to this fact are the continually improving torque and speed control methods of three phase induction motors through semiconductor devices[2].Vector control method of speed control provides precision and wide range qualities simultaneously. The ever-reducing cost of semiconductor devices is making the whole three-phase induction motor drive, an economically better feasible option for a whole number of control and power applications. The scalar control is being replaced by vector control developed almost two decades back. The Direct Vector Control uses the devices like Hall sensors and Search Coils for measuring air-gap flux[3]. This method is problematic in the sense that Hall

ISSN (Online) 2395-2717

International Journal of Engineering Research in Electrical and Electronic Engineering (IJEREEE)
Vol 4, Issue 3, March 2018

sensors are temperature sensitive and fragile while Search Coils have a drift in the integrator attached to it at very low frequency so an Indirect Vector Control was devised. Indirect method does not rely on air-gap flux measurement and instead uses motor parameters for flux calculation [4]. Current controlled VSI is normally used in place of voltage controlled VSI because of the direct control of stator currents (due to fast switching devices and ample dc voltage) than stator voltage which must incorporate additional effects of stator transient inductances [5,6]. The absence of the autonomous inductor device and the lack of rotor currents measurements increase the complexity of the control structure. This control structure must allow creating in the machine an equivalent permanent magnetic through the control of rotor flux, and the decoupling between this flux and the electromagnetic torque. This is why the mathematical models have to describe with the highest possible accuracy the operating of the machine in both steady-state and transient regime [7]. The various PWM techniques utilized in the VSI are analyzed based on. The dynamic modeling of IM is studied from [8,9]. Several modern non-linear control methods used in the control are reported in the literature as feedback linearization techniques or robust techniques based on variable structure systems [10-13]. A deep analysis of the dynamic performance of a closed loop Induction motor drive consisting of hysteretic current controlled VSI based on the field-oriented control is done in [14,15]. It also uses PI controller for speed loop. Any simulation requires the modeling of IM, inverter and controller that is done in using unity power factor converter [16]. The method of determining the stability of a rectifier-inverter induction motor drive system has been used to predict the stability of drive system employing nyquist's criterion. The regions of instability depend upon various system parameters like applied stator voltages, machine parameters, filter parameters and commutating reactance's of the rectifier [17]. A symmetrical induction machine may become unstable at low speeds(low frequencies) even though balanced, constant amplitude sinusoidal voltages are applied to the stator terminals. When machine instability does not occur, regions of lightly damped operation may exit. When the induction machine is furnishing mechanical power to a pulsating load such as a compressor or pump it is of importance to establish the amount of system damping available from the induction machine [18]. The decoupling control between the rotor flux and the torque is no longer achieved in terms of stator current components considering core loss into account. In this paper sinusoidal PWM method is used for control of harmonics and, variation of the fundamental components is achieved by chopping the input voltage to maximize fundamental and selectively eliminate a few lower harmonics [19]. A method to control the IM using flux estimator and speed controller has been used to make the speed control of IM much easier. The amplitude of stator flux is decided by vd, and the electric torque is decided by Vq when the flux amplitude is constant. By adopting two PI controller to regulate flux and electric torque respectively, the V d and Vq can be derived. [20]. A new numerical method for stability analysis with the help of the equations with representative phasors has been recommended. The decreases of the stator winding resistance and rotor resistance decrease the machine stability. While the increase of the stator winding inductivity and rotor inductivity decreases the stability. The inertia moment increase contributes to the stability [21-22].

III. DERIVATION OF INDIRECT VECTOR CONTROL SCHEME

Fig. 1 shows an dynamic de and qe equivalent model of induction motor and the indirect vector controller is derived from the dynamic equations of the induction machine in the synchronously rotating reference frames. The rotor equations of the induction machine containing flux linkages as variables are given by

$$R_r i^{e}_{qr} + p\lambda^{e}_{qr} + \omega_{sl}\lambda^{e}_{dr} = 0 \quad (1)$$

$$R_r i^{e}_{dr} + p\lambda^{e}_{dr} - \omega_{sl}\lambda^{e}_{qr} = 0 \quad (2)$$

Where

$$\omega_{sl} = \omega_s - \omega_r \quad (3)$$

$$\lambda^{e}_{qr} = L_m i^{e}_{qs} + L_r i^{e}_{qr} \quad (4)$$

$$\lambda^{e}_{dr} = L_m i^{e}_{ds} + L_r i^{e}_{dr} \quad (5)$$

Assuming the rotor flux linkages are on direct axis and are a single variable. Hence aligning the d axis with rotor flux phasors gives

$$\lambda_r = \lambda^{e}_{dr} \quad (6)$$

$$\lambda^{e}_{qr} = 0 \quad (7)$$

$$p\lambda^{e}_{qr} = 0 \quad (8)$$

ISSN (Online) 2395-2717

International Journal of Engineering Research in Electrical and Electronic Engineering (IJEREEE)
Vol 4, Issue 3, March 2018

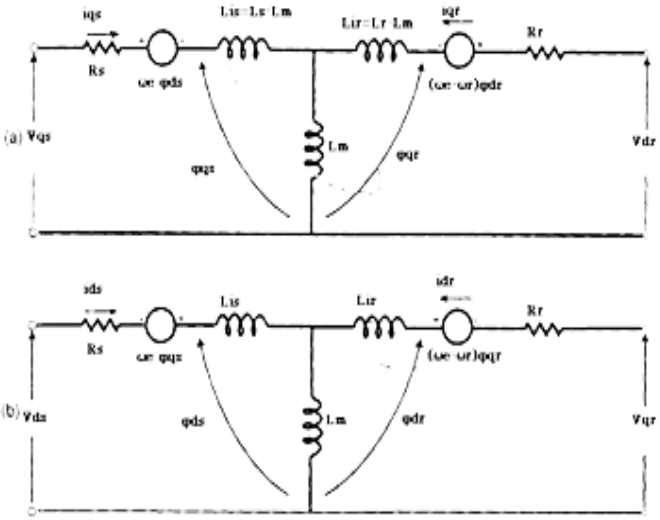

Fig. 1. Dynamic de and qe equivalent model of induction motor.

the (6),(7),(8) gives the new rotor equations are

$$R_r i^e_{qr} + \omega_{sl} \lambda_r = 0 \quad (9)$$

$$R_r i^e_{dr} + p \lambda_r = 0 \quad (10)$$

The rotor current in terms of stator currents are

$$i^e_{qr} = -\frac{L_m}{L_r} i^e_{qs} \quad (11)$$

$$i^e_{dr} = \frac{\lambda_r}{L_r} - \frac{L_m}{L_r} i^e_{ds} \quad (12)$$

Substituting the (11),(12) the following are obtained

$$i_f = \frac{1}{L_m}[1 + T_r p]\lambda_r \quad (13)$$

$$\omega_{sl} = K_{it}\left[\frac{L_r}{T_r}\right]\left[\frac{T_e}{L_r^2}\right] = K_{it} R_r \left[\frac{T_e}{\lambda_r^2}\right] = \frac{L_m}{T_r}\frac{i_T}{\lambda_r} \quad (14)$$

Where $i_f = i^e_{ds}$ (15)

$$i_T = i^e_{qs} \quad (16)$$

$$T_r = \frac{L_r}{R_r} \quad (17)$$

$$K_{it} = \frac{2}{3}\frac{2}{P} \quad (18)$$

The substitution of the rotor currents from (11),(12) into torque expression the electromagnetic torque is derived as

$$T_e = \frac{3}{2}\frac{P}{2}\frac{L_m}{L_r}\left(\lambda^e_{dr} i^e_{qs} - \lambda^e_{qr} i^e_{ds}\right) = \frac{3}{2}\frac{P}{2}\left(\lambda^e_{dr} i^e_{qs}\right) = K_{te}\lambda_r i^e_{qs} = K_{te}\lambda_r i_T \quad (19)$$

The torque constant Kte is define as

$$K_{te} = \frac{3}{2}\frac{P}{2}\frac{L_m}{L_r} \quad (20)$$

The vector controller accepts the torque and flux requests and generates the torque and flux producing components of the stator-current phasor and the slip-angle, θsl, Commands . The command values and the controller-instrumented parameters are denoted with asterisks throughout. From (15),(16),(18) the commanded values of iT, iF, and wsl are

$$i^*_T = \frac{T^*_e}{K_{te}\lambda^*_r} = \frac{T^*_e}{\lambda^*_r}\frac{L^*_r}{L^*_m}\left(\frac{2}{3}\right)\left(\frac{2}{P}\right) = K_{it}\left(\frac{T^*_e}{\lambda^*_r}\right)\left(\frac{L^*_r}{L^*_m}\right) \quad (21)$$

$$i^*_f = \left(1 + T^*_r p\right)\left(\frac{\lambda^*_r}{L^*_m}\right) \quad (22)$$

$$\omega^*_{sl} = K_{it}\left[\frac{L^*_r}{T^*_r}\right]\left[\frac{T^*_e}{(\lambda^*_r)^2}\right] = K_{it} R^*_r \frac{T^*_e}{(\lambda^*_r)^2} = \frac{L^*_m}{T^*_r}\frac{i^*_T}{\lambda^*_r} \quad (23)$$

the stator q and d axis and abc current commands are derived as

$$i^*_{qs} = |i^*_s| \sin\theta^*_s \quad (24)$$

$$i^*_{ds} = |i^*_s| \cos\theta^*_s \quad (25)$$

$$i^*_{as} = |i^*_s| \sin\theta^*_s \quad (26)$$

$$i^*_{bs} = |i^*_s| \sin\left(\theta^*_s - \frac{2}{3}\Pi\right) \quad (27)$$

$$i^*_{cs} = |i^*_s| \sin\left(\theta^*_s + \frac{2}{3}\Pi\right) \quad (28)$$

Where

$$\theta^*_s = \theta_f + \theta^*_T = \theta_r + \theta^*_{sl} + \theta^*_T \quad (29)$$

Design Of Speed Controller

The vector controller transform the induction motor drive into a linear system, even for large signals when the flux linkages are maintained constant and hence resembles the separately excited dc motor drive in all aspects. Following equations gives the systematic development of the transfer function derivation for controlling the speed of induction motor drive. The assumption is, the rotor flux linkages is made constant.

$$\lambda_r = cons\tan t \quad (30)$$

$$p\lambda_r = 0 \quad (31)$$

The stator equations of induction motor are

$$v^e_{qs} = (R_s + L_s p) i^e_{qs} + \omega_s L_s i^e_{ds} + L_m p i^e_{qr} + \omega_s L_m i^e_{dr} \quad (32)$$

$$v^e_{ds} = -\omega_s L_s i^e_{qs} + (R_s + L_s p) i^e_{ds} - \omega_s L_m i^e_{qr} + L_m p i^e_{dr} \quad (33)$$

ISSN (Online) 2395-2717

International Journal of Engineering Research in Electrical and Electronic Engineering (IJEREEE)
Vol 4, Issue 3, March 2018

As d-axis stator current is constant in synchronous frame its derivative is zero.

$$i_f = i_{ds}^e \tag{34}$$

$$p i_{ds}^e = 0 \tag{35}$$

q-axis current in synchronous frame is torque producing component of stator current.

$$i_T = i_{qs}^e \tag{36}$$

Hence

$$v_{qs}^e = (R_s + L_a p) i_T + \omega_s L_a i_f + \omega_s \frac{L_m}{L_r} \lambda_r \tag{37}$$

Where

$$L_a = \sigma L_s = \left(L_s - \frac{L_m^2}{L_r} \right) \tag{38}$$

Substituting

$$\lambda_r = L_m i_f \tag{39}$$

$$v_{qs}^e = (R_s + L_a p) i_T + \omega_s L_a i_f + \omega_s \frac{L_m^2}{L_r} i_f = R_s + L_a p i_T + \omega_s L_s i_f \tag{40}$$

iT is the variable under control in the system. The stator frequency is given as

$$\omega_s = \omega_r + \omega_{sl} = \omega_r + \frac{i_T}{i_f} \left(\frac{R_r}{L_r} \right) \tag{41}$$

Electrical equation of the motor is given by

$$v_{qs}^e = (R_s + L_a p) i_T + \omega_r (L_s i_f) + \omega_{sl} L_s i_f = (R_s + L_a p) i_T + \omega_r (L_s i_f) + i_T \frac{R_r L_s}{L_r} =$$

$$\left(R_s + \frac{R_r L_s}{L_r} L_a p \right) i_T + \omega_r L_s i_f \tag{42}$$

Which gives

$$i_T = \frac{v_{qs}^e - \omega_r L_s i_f}{R_s + \frac{R_r L_s}{R_r} L_a p} = \frac{K_a}{(1 + s T_a)} \left\{ v_{qs}^e - \omega_r L_s i_f \right\} \tag{43}$$

Where

$$R_a = R_s + \frac{L_s}{L_r} R_r \tag{44}$$

$$K_a = \frac{1}{R_a} \tag{45}$$

$$T_a = \frac{L_a}{R_a} \tag{46}$$

From this block voltage and speed feedback converted to electromagnetic torque.

$$T_e = K_t i_T \tag{47}$$

where torque constant

$$K_t = \frac{3}{2} \frac{P}{2} \frac{L_m^2}{L_r} i_f \tag{48}$$

$$J \frac{d\omega_m}{dt} + B \omega_m = T_e - T_1 = K_t i_T - B_l \omega_m \tag{49}$$

In terms of rotor speed

$$J \frac{d\omega_r}{dt} + B \omega_r = \frac{P}{2} K_t i_T - B_l \omega_r \tag{50}$$

The transfer function between speed and torque producing current is given by

$$\frac{I_T}{\omega_r}(s) = \frac{K_m}{1 + s T_m} \tag{51}$$

Where

$$K_m = \frac{p}{2} \frac{K_t}{B_t} \tag{52}$$

$$B_t = B + B_l \tag{53}$$

$$T_m = \frac{J}{B_t} \tag{54}$$

The gain obtained from the dc link voltage Vdc and maximum control voltage Vcm is

$$K_{in} = 0.65 \frac{V_{dc}}{V_{cm}} \tag{55}$$

$$T_{in} = \frac{1}{2 f_c} \tag{56}$$

A proportional plus integral (PI) controller is used to process the speed error between speed reference and filtered speed feedback signals. The transfer function of speed controller is

$$G_s(s) = \frac{K_s}{s} \frac{(1 + s T_s)}{T_s} \tag{57}$$

Current feedback transfer function is

$$G_c(s) = H_c \tag{58}$$

Speed feedback transfer function is process through a first order filter is

$$G_\omega(s) = \frac{\omega_{rm}}{\omega_r}(s) = \frac{H_\omega}{1 + s T_\omega} \tag{59}$$

The loop transfer function of the speed loop is given by

$$GH(s) \cong \frac{K_s}{T_s} K_g \frac{1 + s T_s}{s^2 (1 + s T_{\omega i})} \tag{60}$$

The current loop time constant and speed filter time constant are combine into an equivalent time constant

$$T_{\omega i} = T_\omega + T_i \tag{61}$$

ISSN (Online) 2395-2717

International Journal of Engineering Research in Electrical and Electronic Engineering (IJEREEE)
Vol 4, Issue 3, March 2018

$$K_g = K_i K_m \frac{H_\omega}{T_m} \quad (62)$$

speed controller constants are

$$T_s = 6T_{\omega i} \quad (63)$$

$$K_s = \frac{4}{9}\frac{1}{K_g T_{\omega i}} \quad (64)$$

The proportional and integral gains of the speed controller are obtained as

$$K_s = K_p = \frac{4}{9}\frac{1}{K_g T_{\omega i}} \quad (65)$$

$$K_i = \frac{K_s}{T_s} = \frac{2}{27}\frac{1}{K_g T_{\omega i}^2} \quad (66)$$

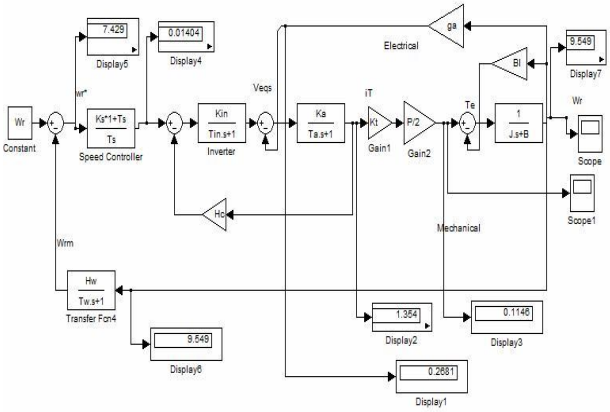

Fig. 2. block diagram of vector controlled induction motor.

V. STABILITY STUDIES

An indirect vector control of induction motor is implemented in this paper, which does not require the use of expensive current sensing devices and Hall Effect sensors in the whole speed control system. An indirect vector controller is designed so that it accepts the requisite torque and flux request and generate the torque and flux producing components of the stator current phasor and the slip angle commands.

A. Dynamic simulation of indirect vector controlled induction motor drive

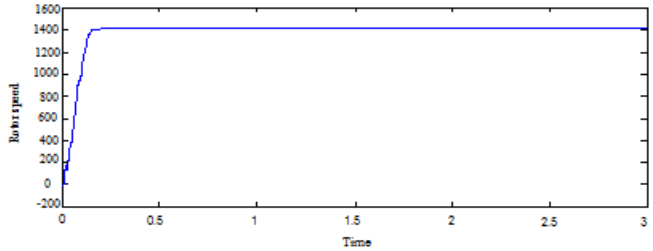

Fig. 3 Rotor speed at full load

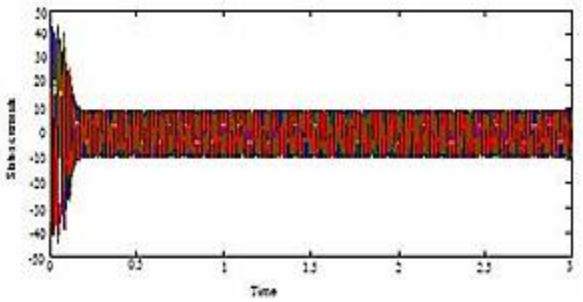

Fig. 4 Stator current at full load.

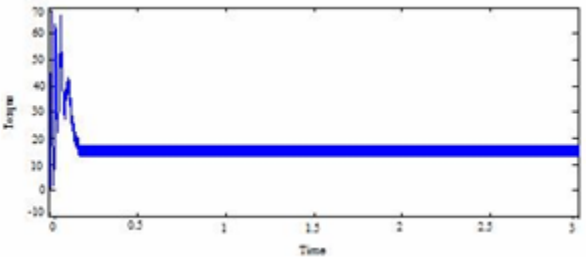

Fig. 5 Torque at full load.

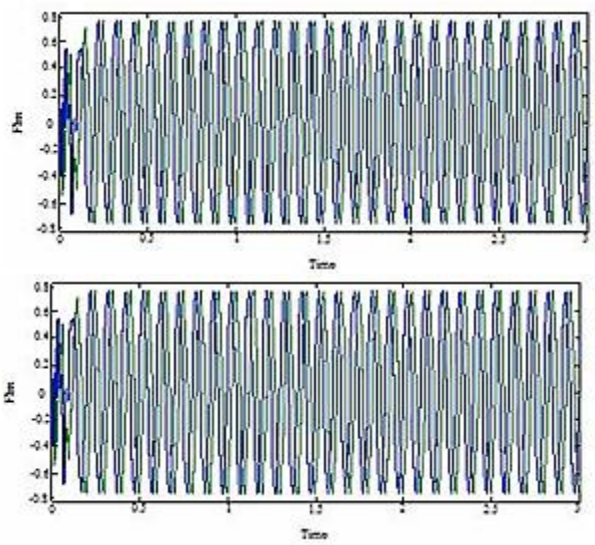

Fig. 6 Flux at full load.

For a step speed reference its response is shown in figure 3 which is very smooth without ripples. The corresponding input currents of stator has been shown in fig 4. The electromagnetic torque command is limited at full load and is almost instantaneous, while rotor flux is at rated value at the time of application of the speed command.

B. Stability Analysis

A change in frequency can be obtain by appropriate changes in the value of fR. in this stability study, 50 Hz is

ISSN (Online) 2395-2717

International Journal of Engineering Research in Electrical and Electronic Engineering (IJEREEE)
Vol 4, Issue 3, March 2018

assumed to be base frequency and the per unit system is based on operation at this frequency(ωb=314.15 rad/sec). Varying modulation index changes the fundamental amplitude of stator voltage and varying the frequency of reference changes the output frequency. For Fc=0.22pu system becomes marginally stable shown in figure 4and for Fc=0.14pu system becomes completely unstable shown in figure 5 as the locus not encircled the (-1+j0).

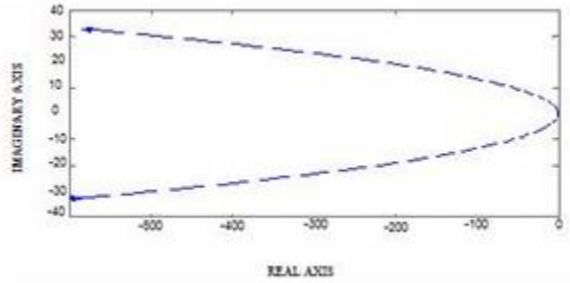

Fig. 7 System is stable for Fc = 21.6 pu.

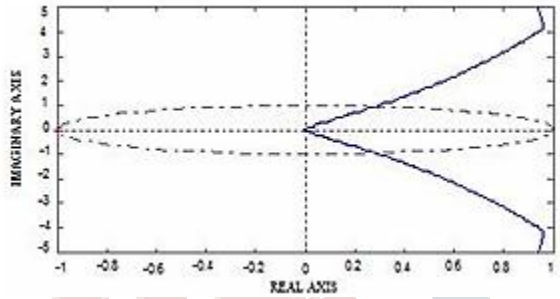

Fig. 8 System is unstable for Fc = 0.08 pu.

C. Variation in parameters

As the load is modeled as a moment of inertia, J(kg=m2/sec2). For any change in the load at the system J is varies and corresponding changes the region of stability in the system.

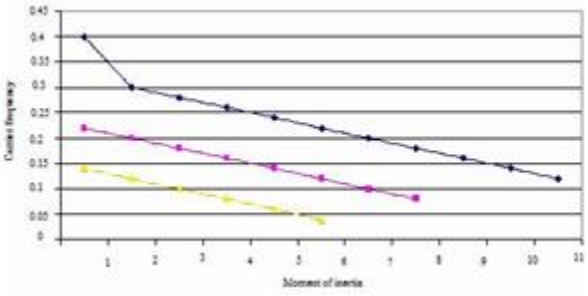

Fig. 9 Variation in moment of inertia J.

From fig. 9 shows the graphical representation of frequencies for variation in moment of inertia. Table I gives the stable and unstable range of frequency in tabular form. Regions of instability obtained from a digital computer study. It is found that stability of system is increase at 0.0404pu compared to 0.03pu, while at 0.05pu system is stable even at lower frequency of 0.04pu. Hence as the J is increased the system will be more stable at lower frequency.

TABLE I

TABLE SHOWING THE RANGE OF FREQUENCY FOR STABLE AND UNSTABLE SYSTEM FOR VARIATION IN MOMENT OF INERTIA

Carrier Frequency(F_c)		J=0.03 pu	J=0.0404pu	J=0.05 pu
Hz	pu			
1080	21.6	stable	stable	stable
1000	20	stable	stable	stable
500	10	stable	stable	stable
400	8	stable	stable	stable
300	6	stable	stable	stable
200	4	stable	stable	stable
100	2	stable	stable	stable
90	1.8	stable	stable	stable
80	1.6	stable	stable	stable
70	1.4	stable	stable	stable
60	1.2	stable	stable	stable
50	1	stable	stable	stable
40	0.8	stable	stable	stable
30	0.6	stable	stable	stable
20	0.4	Mstable	stable	stable
15	0.3	Mstable	stable	stable
14	0.28	Mstable	stable	stable
13	0.26	Mstable	stable	stable
12	0.24	Mstable	stable	stable
11	0.22	Mstable	Mstable	stable
10	0.2	Mstable	Mstable	stable
9	0.18	Mstable	Mstable	stable
8	0.16	Mstable	Mstable	stable
7	0.14	Mstable	Mstable	Mstable
6	0.12	Unstable	Mstable	Mstable
5	0.1		Mstable	Mstable
4	0.08		Unstable	Mstable
3	0.06			Mstable
2	0.04			stable

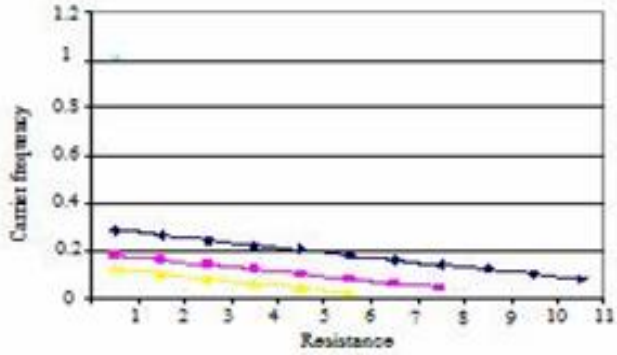

Fig. 10 Variation in resistance Ra.

ISSN (Online) 2395-2717

International Journal of Engineering Research in Electrical and Electronic Engineering (IJEREEE)
Vol 4, Issue 3, March 2018

TABLE II
TABLE SHOWING THE RANGE OF FREQUENCY FOR STABLE AND UNSTABLE SYSTEM FOR VARIATION IN RESISTANCE

Carrier Frequency (F_c)		Ra=0.02 pu	Ra=0.05 pu	Ra=0.06 pu
Hz	pu	stable	stable	stable
20	0.4	stable	stable	stable
19	0.38	stable	stable	stable
18	0.36	Stable	Stable	Stable
17	0.34	Stable	Stable	Stable
16	0.32	Stable	Stable	Stable
15	0.3	Stable	Stable	Stable
14	0.28	Mstable	Stable	Stable
13	0.26	Mstable	Stable	Stable
12	0.24	Mstable	stable	stable
11	0.22	Mstable	stable	stable
10	0.2	Mstable	stable	stable
9	0.18	Mstable	Mstable	stable
8	0.16	Mstable	Mstable	stable
7	0.14	Mstable	Mstable	stable
6	0.12	Mstable	Mstable	Mstable
5	0.1	Mstable	Mstable	Mstable
4	0.08	Unstable	Mstable	Mstable
3	0.06		Mstable	Mstable
2	0.04		Unstable	Mstable
1	0.02			Mstable

Fig. 10 and Table II indicate the region of instability. Decrease in resistance decreases the stability in system, vice versa. At 0.02pu system becomes marginally unstable at frequency of 0.28pu while becomes completely unstable at frequency of 0.08pu. As the resistance is increase at 0.05pu, system becomes marginally unstable at frequency of 0.18pu while it becomes completely unstable at frequency of 0.04pu.

A small variation in inductance of the machine makes the changes in the stability of system.

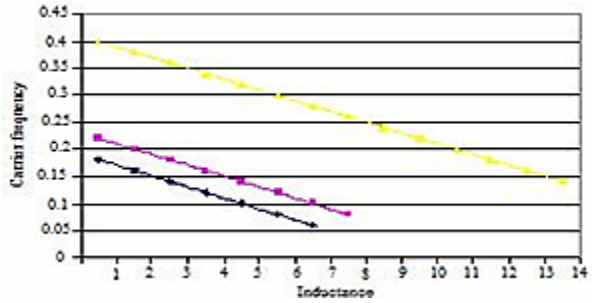

Fig. 11 Variation inductance La.

TABLE III
TABLE SHOWING THE RANGE OF FREQUENCY FOR STABLE AND UNSTABLE SYSTEM FOR VARIATION IN INDUCTANCE

Carrier frequency (F_c)		La=0.07pu	La=0.09pu	La=0.2pu
Hz	Pu			
20	0.4	Stable	Stable	Mstable
19	0.38	Stable	Stable	Mstable
18	0.36	Stable	Stable	Mstable
17	0.34	Stable	Stable	Mstable
16	0.32	Stable	Stable	Mstable
15	0.3	Stable	Stable	Mstable
14	0.28	Stable	Stable	Mstable
13	0.26	Stable	Stable	Mstable
12	0.24	Stable	Stable	Mstable
11	0.22	Stable	Mstable	Mstable
10	0.2	Stable	Mstable	Mstable
9	0.18	Mstable	Mstable	Mstable
8	0.16	Mstable	Mstable	Mstable
7	0.14	Mstable	Mstable	Unstable
6	0.12	Mstable	Mstable	
5	0.1	Mstable	Mstable	
4	0.08	Mstable	Unstable	
3	0.06	Unstable		
2	0.04			
1	0.02			

From fig. 11 and table III the region of instability for inductance of 0.07pu is small as compared to 0.09pu, while inductance of 0.2pu increases the region of instability more than at 0.07pu and 0.09pu. As the inductivity increase the stability of system decreases.

VI. CONCLUSION

This paper has presented indirect vector control system for induction motor drives and its stability study. The simulation results showed that the performance of the induction motor is exactly the same as the separately excited dc motor having also a quick dynamic response and low torque pulsation. It clarifies that the stability problem is an inherent aspect in an induction motor. A few interesting results regarding the induction motor parameters influences on the dynamic regime behavior of the analyzed driving system. The decrease of the stator winding resistance and rotor resistance decrease the machine stability. Also the increase of stator winding inductivity and rotor inductivity decrease the system stability. An increment in the moment of inertia contributes to increase the stability.

REFERENCES

Periodicals:

[1] Z. S. Wang & S. L. HO, "Indirect rotor field orientation vector control for induction motor drives in the absence of current sensors," IEEE Trans industry Applications, Vol. No I , pp 4244-4249.

[2] Alexandru Onea, Vasile Hogra, Marcel Ratoi, "Indirect vector control of induction motor," Proc. of 6th WSEAS International conference on simulation & Modeling and optimization,Lisban,Portugal, September 2006.

[3] A Shiri , A Vahedi & A.Shoulare," The effect of parameter variations on the performance of indirect vector controlled induction motor drive," IEEE ISIE July 9-12, Montreal, Canada.

[4] Anurag Tripathi, Arunima Dey, Bharti dwivedi, Bhim Singh, Dinesh Chandra, "A new closed loop speed control strategy for a vector controlled three phase induction motor drive," Electrical Power Quality and utilization, Journal Vol. XIV, No 1, 2008

[5] G. Esmaily (M.Sc.), A. Khodabakhshian (Ph.D), K. Jamshidi (Ph.D)."
Vectot control of induction motors using upwm voltage source invertor" isfahan university, Iran.

[6] M.P. Kazmierkowski, "A novel vector control scheme for transistor PWM inverter-fed induction motor drive" , IEEE Trans. On indust. Vol. 38, No.1, Feb 1991, pp. 41-47

[7] O. Barambones, A.J. Garrido and F.J. Maseda," A Sensorless Robust Vector Control of Induction Motor Drives."

[8] Yury Kolokolov, Artem Melikhov, Abdelaziz Hamzaoui, Najib Essounbouli, Janan Zaytoon, "Stability Analysis of a "Thyristor Voltage Controller –Induction Machine Model."

[9] Janne Salomäki and Jorma Luomi," Vector Control of an Induction Motor Fed by a PWM Inverter with Output LC Filter."

[10] H.Altun and S.Sünter, "Simulation and Modelling of Vector Controlled 3-Phase Matrix Converter Induction Motor Drive" ELECO'01, Bursa, Nov. 7-11, 2001, pp .98-102.

[11] Sergei Peresada , Andrea Tilli , Sergei Kovbasa , Marcello Montanari and Fabio Ronchi," Simple Sensorless Vector Control of Induction Motors with Natural Field Orientation."

[12] Yi Wang, Heming Li, Xinchun Shi." Direct Torque Control with Space Vector Modulation for Induction Motors Fed by Cascaded Multilevel Inverters."

[13] Mohammad. Abdul Mannan, Toshiaki Murata, Junji Tamura, "Indirect Field Oriented Control for High Performance Induction Motor Drives Using Space Vector Modulation with consideration of Core Loss."0-7803-7754,2003IEEE.

[14] Thomas A. Lipo, member, IEEE, and Paul C. Krause, senior member, IEEE "Stability analysis of a rectifier- Inverter Induction Motor Drive" IEEE transaction on power apparatus, VOL. PAS-88, No. 1, January 1969.

[15] Robert H. Nelson, Thomas A. Lipo, member, IEEE, and Paul C. Krause, senior member, IEEE "Stability Analysis of a Symmetrical Induction Machine" IEEE vol., PAS-88, No. 11, November1969.

[16] Monica, Adela enache, Sorin Enache, Mircea Dobriceanu"Effects of induction motors inductances modification on stabilityanalyzed with numerical methods" International general of mathematics and computers in simulation issue 2, volume 1,2007.

[17] Sorin Enache, Aurel Campeanu, Ion Vlad, Monica Adela Enache "Implementation of a Numerical Method for the stability Analysis of Asynchronous Motors Operating at Variable Frequency" International General of mathematical models and Methods in Applied Sciences. Issue 4, volume 1, 2007.

[18] S. Jagtap, S. Muley and M. Aware, "Harmonic analysis in vector controlled variable frequency drive", presented at the Harmonica-09, Institute of engineers, Nagpur, India.

[19] S. Jagtap, S. Muley and M. Aware, "An indirect vector controlled voltage source inverter induction motor drive", presented at the NCAPS-09, K. K. Wagh institute of engineering education and research, Nashik-03, India.

Books:

[20] P. S. Bhimra, " Generalized theory of electrical machines".

[21] B. K. Bose, " Modern power electronics and AC drives," LPE, Pearson, Ed. New Delhi.

[22] R. Krishnan,"Electric motor drive : Modeling, Analysis, and Control"
.LPE,Pearson Ed. New Delhi..